References

BEGER, R. M. (1969). *Z. Krist.* **129**, 280–302.

BELL, A. M. T., HENDERSON, C. M. B., REDFERN, S. A. T., CERNICK, R. J., CHAMPNESS, P. E., FITCH, A. N. & KOHN, S. C. (1994). *Acta Cryst.* B**50**, 31–41.

BOYSEN, H. (1990). Phase transitions in ferroelastic and coelastic crystals. In *Cambridge Topics in Mineral Physics and Chemistry*, edited by E. K. H. SALJE, pp. 334–349. Cambridge: Cambridge University Press.

CERNIK, R. J., MURRAY, P. K., PATTISON, P. & FITCH, A. N. (1990). *J. Appl. Cryst.* **23**, 292–296.

COLLINS, S. P., CERNIK, R. J., PATTISON, P., BELL, A. M. T. & FITCH, A. N. (1992). *Rev. Sci. Instrum.* **63**(1), 1013–1014.

DUPREE, R., KOHN, S. C., HENDERSON, C. M. B. & BELL, A. M. T. (1992). Calculation of NMR shielding constants and their use in the determination of the geometric and electronic structures of molecules and solids, edited by J. A. TOSSELL, NATO A.S.I. Vol., pp. 421–430.

HEINRICH, A. R. & BAERLOCHER, CH. (1991). *Acta Cryst.* C**47**, 237–241.

HILL, R. J. & GIBBS, G. V. (1979). *Acta Cryst.* B**35**, 25–30.

KOHN, S. C., DUPREE, R., MORTUZA, M. G. & HENDERSON, C. M. B. (1991). *Phys. Chem. Miner.* **18**, 144–152.

KOHN, S. C., HENDERSON, C. M. B. & DUPREE, R. (1994). *Phys. Chem. Miner.*, **21**. In the press.

LANGE, R. A., CARMICHAEL, I. S. E. & STEBBINS, J. F. (1986). *Am. Mineral.* **71**, 937–945.

MAZZI, F., GALLI, E. & GOTTARDI, G. (1976). *Am. Mineral.* **61**, 108–115.

MURRAY, A. D., COCKCROFT, J. K. & FITCH, A. N. (1990). Powder Diffraction Program Library (PDPL). Univ. College, London.

PALMER, D. C. (1990). Phase transitions in leucite. PhD Thesis, Cambridge Univ.

PAWLEY, G. S. (1972). *Advances in Structure Research by Diffraction Methods*, edited by W. HOPPE & R. MASON, Vol. 4, pp. 1–64. Oxford: Pergamon Press.

RIETVELD, H. M. (1969). *J. Appl. Cryst.* **2**, 65–71.

ROBINSON, K., GIBBS, G. V. & RIBBE, P. H. (1971). *Science*, **172**, 567–570.

ROLLET, J. S. (1970). *Crystallographic Computing*, edited by F. R. AHMED, p. 170. Copenhagen: Munksgaard.

SHANNON, R. D. (1976). *Acta Cryst.* A**32**, 751–767.

TORRES-MARTINEZ, L. M. & WEST, A. R. (1989). *Z. Anorg. Allg. Chem.* **573**, 223–230.

High-Resolution Neutron Study of Vitamin B_{12} Coenzyme at 15 K: Solvent Structure

BY J. P. BOUQUIERE

Crystallography Department, Birkbeck College, Malet Street, London WC1E 7HX, England

J. L. FINNEY

Department of Physics and Astronomy, University College London, Gower Street, London WC1E 6BT, England

AND H. F. J. SAVAGE

Chemistry Department, York University, Heslington YO1 5DD, England

This paper is dedicated to the memory of the recent loss of Dr E. Lester Smith, a pioneer in the isolation of vitamin B_{12}

Abstract

The solvent structure of crystalline vitamin B_{12} coenzyme, determined from a high-resolution (0.9 Å) neutron data set collected at 15 K, is presented. The study involved the identification of solvent peaks and the formulation of possible solvent networks. The solvent distribution within the crystal can be described in two regions, namely (*a*) a channel, comprizing statically disordered water molecules and (*b*) leading into this channel, a region of highly ordered water molecules. The identification of the disordered solvent peaks has enabled the formulation of two main solvent networks per asymmetric unit, with the assistance of criteria used in the analyses of solvent structures in crystal hydrates of small molecules. The two networks comprise 17 water molecules each. A comparison of these solvent networks is made with those identified in a previous study of a crystal of the coenzyme at 279 K. The covalent and hydrogen-bond geometries involving the water molecules of these networks have been analysed and agree well with those found in small molecular crystal hydrates. Furthermore, the analysis of the water structure around apolar groups of the B_{12} coenzyme indicates the presence of clathrate-like water structures, as well as short distances which others have identified as C—H$\cdots$O hydrogen bonds. Short range O$\cdots$O non-hydrogen-bonded contacts obey known repulsive

restriction rules formulated from small-molecule hydrate crystals.

1. Introduction

The structure and function of a biological molecule may be highly dependent on its interactions with the surrounding solvent. For example, the first enzyme structure solved using X-ray diffraction techniques, lysozyme, highlighted the importance of water in the catalytic mechanism (Phillips, 1966). Replacing a polar amino acid residue by an apolar one can give rise to conformational changes that can render the molecule ineffective. Thus, for deoxygenated haemoglobin S, substituting glutamate 6 in the chain by a valine reduces the solubility, giving rise to sickle cell anaemia. Detailed knowledge of the interactions of individual water molecules with chemical groups encountered in proteins and nucleic acids (amides, hydroxyls, methyls, nucleosides etc.) may lead to a better understanding of the macromolecular changes that can occur as a consequence of changes in these interactions. There are several techniques available to study solvent in and around biological molecules, and the choice depends on the property under investigation: dynamic properties are best studied by NMR, IR or inelastic neutron scattering, whereas positional parameters are best determined with the use of elastic diffraction techniques. The oxygen sites of the most highly ordered water molecules can be readily identified in difference X-ray Fourier electron-density maps at resolutions around 2.5 Å, yet for a complete analysis of the solvent, high-resolution data (ideally to at least 1 Å) is essential to be able to locate unambiguously all the atoms involved (including hydrogens). Few X-ray diffraction studies of proteins have approached this level of resolution, with the exception of certain small polypeptides and proteins such as crambin with 46 amino-acid residues to 0.83 Å resolution (Teeter & Hope, 1986), rubredoxin with 52 amino-acid residues to 1.0 Å resolution (Dauter, Sieker & Wilson, 1992) and γB-crystallin, 174 residues to 1.2 Å (Lindley et al., 1993)

Neutron diffraction enables all atoms to be characterized as they have roughly the same absolute scattering lengths. However, the aquisition of good data is dependent on the production of large crystals (5 mm³); relatively few proteins have crystals of this size at present. Neutron data for lysozyme have been refined to 1.4 Å (Mason, Bentley & McIntyre, 1984) and for crambin to 1.1 Å resolution (Teeter & Whitlow, 1986). In an attempt to construct a picture of water interactions with chemical groups of biological relevance, various workers have reviewed the neutron diffraction studies of crystal hydrates of small molecules [amino acids and carbohydrates (Chiari & Ferraris, 1982; Jeffrey & Maluszynska, 1990; Steiner & Saenger, 1993)]. These crystal hydrates only contain a few water molecules each (typically 2–4), which thus provides only a limited picture of the interactions of the ordered solvent within macromolecular crystals; they are insufficiently hydrated to reveal the complex nature of the bulk, or disordered, solvent networks that extend throughout the crystals.

To be able to characterize more fully the disordered networks, it is advisable to collect the data at low temperatures. β-Cyclodextrin has been studied at very high resolution and at various temperatures using neutron diffraction techniques: 293 (Betzel, Saenger, Hingerty & Brown, 1984), 120 (Zabel, Saenger & Mason, 1986), 15 (Steiner, Mason & Saenger, 1990) and 295 K (Steiner, Mason & Saenger, 1991). The crystals contain 8–11 water molecules per asymmetric unit. Models for the study of water interactions with proteins and nucleic acids should include a variety of chemical groups, such as those encountered in these macromolecules (amides, methyls, riboses etc.). Vitamin B_{12} coenzyme ($C_{72}H_{100}CoN_{18}O_{17}P$) is a particularly useful model compound as it possesses a number of chemical
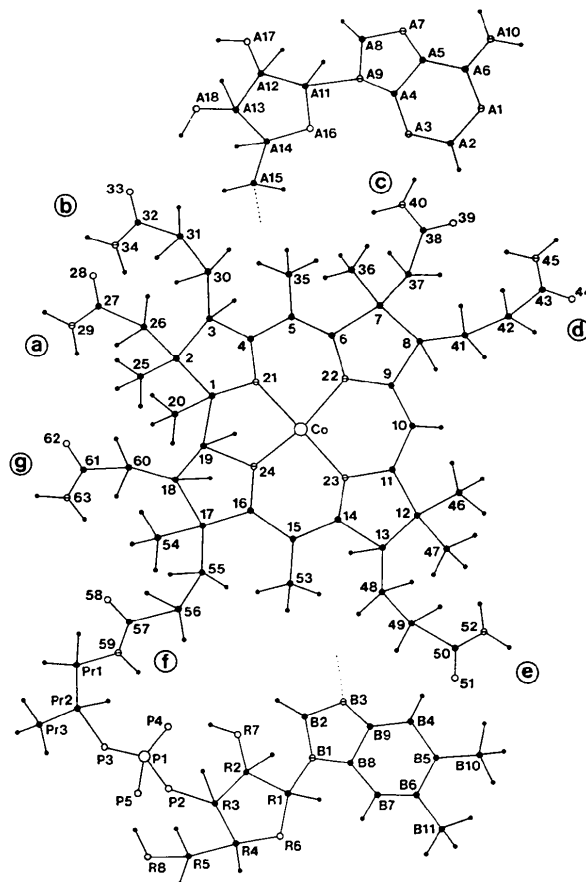

Fig. 1. Atom labelling for vitamin B_{12} coenzyme molecule for non-H atoms: filled circles, C; open circles (small), O: open circles with horizontal lines, N; open circles (large), Co and P. The side chains are labelled by circled letters a–g. The dotted lines represent the bonds between the nitrogen B3 and the central Co atom, and between the carbon A15 and the Co.

groups found in biological macromolecules and is larger than cyclodextrins. It has 209 atoms ($M_r = 1578$), 17–18 water molecules per asymmetric unit (70 per unit cell) and it is large enough to present a sizeable interface to the solvent. It contains a porphyrin-like ring, methyl and amide groups, a nucleotide and a nucleoside (see Fig. 1). It also has the advantage that large crystals can be grown for single-crystal neutron diffraction.

Savage, Lindley, Finney & Timmins (1987) carried out a neutron study on the coenzyme at 279 K to a resolution of 0.95 Å and identified 17 waters per asymmetric unit; this study led to the identification of several water networks within the crystal and Savage (1986a) was able to highlight the importance of non-bonding O···H and H···H interactions within the water networks. The present paper results from a structural study of the coenzyme using neutrons at 15 K (Bouquiere, Finney, Lehmann, Lindley & Savage, 1993). The water networks are clarified and compared with those at 279 K. At 15 K, the dynamic disorder of the coenzyme molecule and of the waters is expected to be greatly reduced, thus enabling a more detailed analysis of the structural details.

2. Summary of data collection and refinement

Crystals of vitamin B₁₂ coenzyme were grown in D₂O and acetone (Bouquiere, Finney, Lehmann, Lindley & Savage, 1993). A high-resolution neutron data set was collected to 0.90 Å from a single large crystal on the D19 diffractometer at the high flux reactor of the Institut Laue-Langevin, Grenoble, France. The crystal was mounted in a quartz capillary tube and placed within a helium cryostat mounted on the circle of the diffractometer and was slowly cooled to 15 K. The data were collected at $\lambda = 1.5446$ Å to a nominal resolution of 0.98 Å, and then $\lambda = 1.3169$ Å to a nominal resolution of 0.90 Å.

The atomic positions determined at 279 K by Savage, Lindley, Finney & Timmins (1987) were used as the starting model for the current refinement; no solvent atoms from that data set were included. The refinement was carried out in two stages: to 1.0 Å, treating the coenzyme as a small macromolecule, using the macromolecular refinement program *RESTRAIN* (Driessen *et al.*, 1989), at which stage 42 solvent sites were incorporated into the refinement model after examination of ($F_{obs} - F_{calc}$) difference Fourier maps; to 0.9 Å, treating the coenzyme as a large small molecule, using *SHELX76* (Sheldrick, 1976), where a further 25 atom sites were identified from difference Fourier maps. Isotropic thermal parameters were calculated for the solvent atoms ($n = 67$, 23 O atoms and 44 H atoms) and the 19 exchangeable H atoms on the coenzyme molecule, and anisotropic thermal parameters calculated for the remaining 190 coenzyme atoms. Initial occupancies were assessed from solvent peak shapes and

heights from ($F_{obs} - F_{calc}$) difference Fourier maps, with solvent atoms excluded from the model. The occupancies and temperature factors for solvent atoms were refined in alternate cycles. Covalent bond-length restraints of 0.96 Å (0.03 Å) were applied to the disordered water molecules. The final R-factor is 0.081 for all data. Details of the data collection and refinement are given in Bouquiere, Finney, Lehmann, Lindley & Savage (1993). Crystal parameters: $P2_12_12_1$, $a = 27.55$, $b = 21.57$, $c = 15.34$ Å, $Z = 4$, $D_x = 1.38$ Mg m⁻³.

3. Molecular structure of vitamin B₁₂ coenzyme

The coenzyme B₁₂ molecule has a corrin ring at its core with a central Co atom (see Fig. 1). Three acetamides, three propionamides, one propionic acid and eight methyl residues are attached to this porphyrin-like ring. A 5,6-dimethylbenzimidazole is linked to a ribose-3′-phosphate *via* an α-N glycosyl bond, and is located beneath the corrin ring plane; the nucleotide is bonded to the propionic group *via* the phosphate and to the cobalt *via* the second N atom on the benzimidazole. The nucleoside is a 5′-deoxyadenosyl and is situated above the corrin ring; it is linked to the cobalt *via* C5 of the ribose by a Co—C σ-bond.

The differences between the structures at 15 and 279 K involve the unit-cell size, the orientation of the coenzyme in the crystal and the atomic thermal parameters. There has been a 2% shrinkage in unit-cell volume in going from 279 to 15 K and a 2° rotation about an axis almost parallel to the *c* axis of the unit cell and passing close to the Co atom. The average atomic thermal parameters at 15 K are $U_{eq} = 0.016$ Å² and at 279 K, $U_{eq} = 0.040$ Å² for non-solvent and non-H atoms. The other major difference is that at 15 K, there is a major hydrogen content where deuterium was expected: although the technique used for growing the crystals was the same as for the 279 K data, it is possible that there was inadequate sealing between the crystallization vessel and the surrounding atmosphere.

4. Solvent analysis

4.1. Solvent distribution in the crystals

The distribution of the solvent regions within the unit cell of the crystal is shown schematically in Fig. 2. The solvent distribution consists of (a) a channel, comprising statically disordered water molecules, extending throughout the crystal and parallel to the twofold screw axes along the *c* axis of the unit cell at $x = 1/4$, $y = 1/4$ and $x = 3/4$, $y = 0$, and (b) leading into this channel, a region of ordered waters, that is with little or no apparent static and dynamic disorder (the pocket region). The transition from order to disorder is provided by an interface region consisting of a small number of solvent molecules.

4.2. Density analysis

The solvent density in the 15 K structure compared with the 279 K solvent density is much improved [see Figs. 3(a) and (b)] and more readily interpretable for two main reasons. Firstly, at low temperature the peak densities are much sharper and the dynamic disorder reduced, giving rise to better precision of the solvent positions. In particular, this can be seen in the channel region. The solvent density in the 279 K structure is mostly continuous and reasonable water positions were difficult to locate [Fig. 3(b)]. Secondly, the expected positive deuterium solvent peaks were found to be negative hydrogen peaks [Fig. 3(a)]. As stated above, the crystals were originally grown in 99.8% D_2O solution, whereby all solvent peaks were expected to be positive. This made distinguishing between oxygen and deuterium solvent atoms difficult in the 279 K neutron analysis [Fig. 3(b)]. The unexpected presence of solvent hydrogens made the solvent interpretation of the 15 K data very much easier.

4.3. Pocket region

The ($F_{obs} - F_{calc}$) difference Fourier maps, with solvent atoms excluded from the model, identified seven clear positive peaks (oxygens) with their associated negative peaks (hydrogens) in the pocket region. These were waters 211, 212, 213, 223, 216, 217 and 418 [Fig. 3(a)]. There is no evidence of any major static or dynamic disorder for these water positions and they were all assigned unit occupancies during the least-squares refinement.

In the 279 K neutron model, the acetamide c side chain containing the N40 atom was found to be disordered between two main positions [with occupancies of 0.74 (N40) and 0.26 (N640)]. In the 15 K neutron model, only one position is present with unit occupancy corresponding to the higher occupied position in the 279 K model, and water 212 appears fully ordered at 15 K.
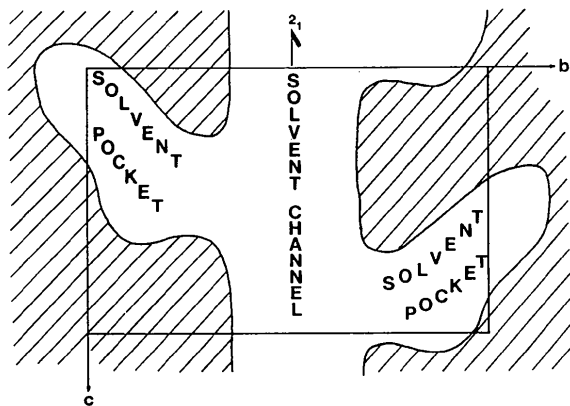
4.4. Interface region

In the 279 K analysis (Savage, 1986a), an acetone molecule with an occupancy of 0.6 was found in a position between the pocket and the channel regions [Fig. 3(b), between waters 216 and 215]. The acetone molecule separated the water network structures into two isolated regions – the pocket and the channel. In this 15 K analysis, an acetone molecule was located, but with a very low occupancy of 0.15. Continuous water network structures can be seen that pass from the pocket region, over the interface region and into the channel.

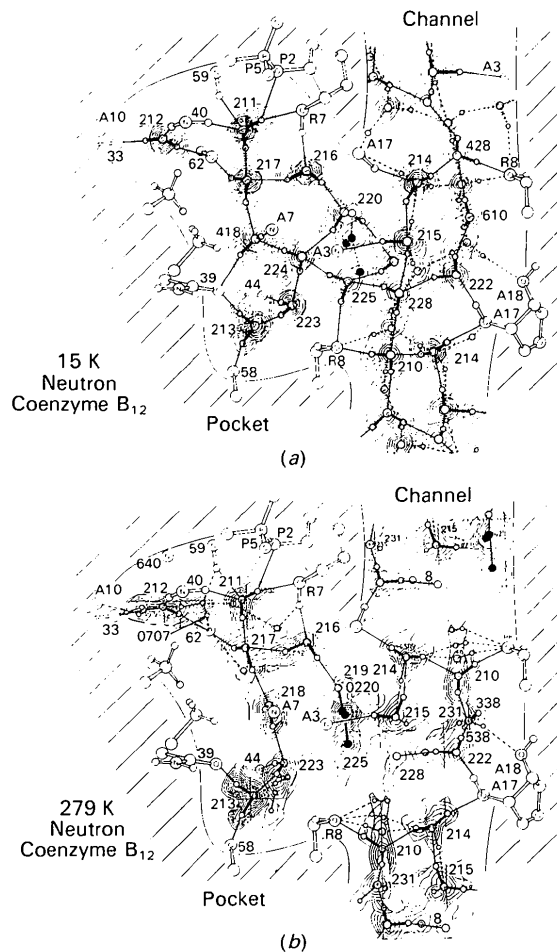The following water positions were assigned to this region: 220, 224, 225 and 426 [see Figs. 3(a), 4(a) and

Fig. 3. Composite maps of the water networks in the B_{12} coenzyme crystal and the neutron ($F_{obs} - F_{calc}$) difference maps (no solvent included as part of the model). Contour levels at 1 r.m.s. Large open circles, O; small open circles, H. Solid and dashed lines between the solvent molecules represent alternative water networks. (a) 15 K – dashed contour lines are negative neutron-density levels, solid contour lines are positive neutron-density levels; the acetone C atoms are represented by filled circles between waters 220 and 225. (b) 279 K – Neutron density is represented by positive contour levels (solid lines) only, as the sample was fully deuterated; the acetone C atoms are represented by filled circles between waters 218 and 215.

Fig. 2. Solvent distribution in the crystal, viewed down the a axis (projection of 1/4 of the bc plane). Shaded areas represent the coenzyme molecules.

(b)]. Their respective occupancies were refined and range from 0.28 to 0.55 for the oxygens and 0.15 to 0.72 for the hydrogens.

4.5. Channel region

Both the channel and interface regions were found to be substantially disordered at 279 K (Savage, 1986a) and the initial difference Fourier maps confirmed that disorder was still present at 15 K. The analysis of solvent density in these regions involved a substantial amount of refinement of the positional, thermal and occupancy parameters.

The following water positions were assigned in this region: 214, 215, 222, 422, 228, 428, 431, 210, 610, 427, 227 and 231 [Figs. 3(a), 4(a) and (b)]. Their refined occupancies ranged from 0.24 to 0.97 for oxygens and

from 0.28 to 0.81 for hydrogens. Three of the water hydrogen sites appear to be shared between two adjacent (mutually exclusive) water oxygens. These are the following hydrogens:

H2 of water 210 between oxygens 210 and 610,
H1 of water 228 between oxygens 228 and 428 and
H2 of water 431 between oxygens 222 and 431.

Water oxygens 210 and 228 are labelled in Fig. 3(a) and oxygens of water 610 and 428 are 2.0 Å vertically below in the plane of the figure. Additional evidence that these hydrogens are shared is the fact that their occupancy values are significantly higher than either of the water oxygens they are covalently bonded to, and higher than the other (unshared) hydrogens on these waters.

5. Criteria for formulation of water networks

Water networks were assigned between the 67 assigned solvent sites using essentially the same criteria as in the 279 K analysis (Savage, 1986a):

(i) Hydrogen bonds were assigned between solvent oxygen and either polar atoms of the coenzyme B$_{12}$ molecule or other solvent oxygen sites for distances between the limits of 2.5 and 3.6 Å. The latter distance appears to be rather longer than the limit usually used in other small molecule hydrogen-bond analyses, for example, 3.3 Å (from Chiari & Ferraris, 1982). However, several longer apparent hydrogen bonds of up to 3.5 Å were observed with the respective H atoms located close to linearity in the hydrogen bond. In these cases, no other alternative hydrogen-bonding geometry for hydrogen is available.

(ii) Water sites were accepted where the $X \cdots O(W) \cdots Y$ hydrogen-bond angles subtended at the water oxygens were within the limits 69 and 148°, found in small crystal hydrates (Chiari & Ferraris, 1982).

(iii) Where mutually exclusive sites occurred (O atoms < 2.6 Å apart), alternative networks were formulated.

(iv) Where possible, water networks were formulated in which the water oxygen sites had similar values.

(v) Networks were also checked for the presence of the acetone molecule. In this paper, networks were formulated for the case of no acetone present.

(vi) Non-bonded $H \cdots H$ distances of less than 2.0 Å were disallowed.

6. Water networks

Using the above criteria, two main water networks could be formulated in each asymmetric unit, without the difficulties that were experienced in the 279 K analysis. These difficulties were namely (a) the identity of solvent peaks greater than 2.8 Å from coenzyme atoms [were they deuterium or oxygen? see Fig. 3(b)] and (b) the greater disorder [cf. Figs. 3(a) and (b)]. The two main

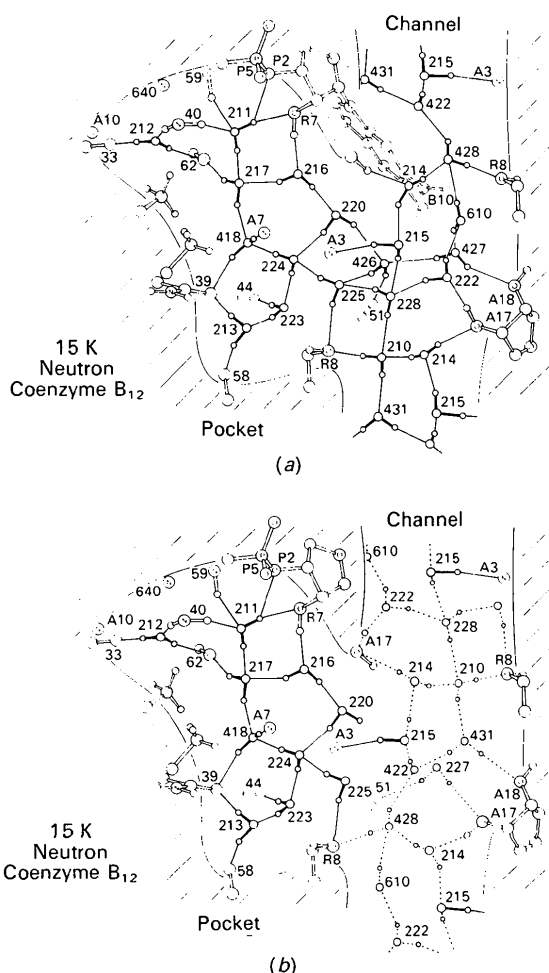Fig. 4. Water networks in the coenzyme crystal at 15 K. (a) Network 1: represented by solid lines between solvent molecules [as in Fig. 3(a)]. Partial clathrate cage of water molecules around the CB10 methyl of the benzimidazole group, which extends into the lower part of the channel region. (b) Network 2: represented by solid lines between waters in the pocket region and dashed lines in the channel region [as in Fig. 3(b)].

networks in the 15 K model are labelled 1 [Fig. 4(a)] and 2 [Fig. 4(b)], which are different labels than those used in the 279 K analysis where they were given the letter labels A–J. Many of the positions are found to be almost the same in the 15 and 279 K structures. These include the following waters (279 K equivalent positions are in parentheses):

211, 212, 213, 223, 216, 217, 220, 214, 215, 222, 210 (410), 226, 227, 231 and 431.

The low-temperature 15 K data, however, have allowed a much better and clearer interpretation of the water network structures. From the two main networks isolated (1 and 2), we are now able to incorporate the networks A–J from the previous analysis. Here we describe the two main water networks, which appear to be present when the acetone position is unoccupied.

The two main networks each contain 17 water positions per asymmetric unit:

Network 1
Pocket region: 211, 212, 213, 216, 217, 418, 223
Interface region: 224, 220, 225, 426
Channel region: 214, 215, 610, 222, 427, 228

Network 2
Pocket region: 211, 212, 213, 216, 217, 418, 223
Interface region: 224, 220, 225
Channel region: 214, 215, 210, 431, 422, 227, 428

With respect to the location and presence of the expected two hydrogen positions for each water oxygen, each network contains 33 H atoms out of the 34 expected. The missing H atom in network 1 belongs to water 215 and could not be clearly located in the difference solvent maps. Some disorder appears to occur between waters 215 (part of network 1) and 422 (part of network 2).

Where the two oxygen sites of a water–water hydrogen bond are well ordered, partially occupied hydrogen sites are often observed between the oxygens. An example of this is seen in Fig. 3(a) between waters 214 and 215, where two hydrogen peaks are present. However, for the case between 215 and 228, there is only one hydrogen peak which is very ellipsoidal, with the longest axis parallel to the 215–228 vector. The 215–228 hydrogen bond lies quite close to a vertical direction in Fig. 3(a) and the density of the hydrogen between them is obscured by the oxygen of water 215. A theoretical hydrogen position was placed on water 215 (third H atom of water 215) pointing to water 228.

In network 2, one H atom of water 422 could not be located in the solvent-density analysis.

Further refinement of this and other regions is being undertaken.

In network 1, all the H atoms participate in hydrogen-bond interactions to either adjacent waters or local coenzyme polar atoms. In network 2, all except two H atoms participate in local hydrogen bonds. The two that do not form hydrogen bonds belong to waters 220 and 422. These waters lie in the disordered interface solvent region between the pocket and the channel in Fig. 3(a). The individual hydrogen-bond geometries are given in Table 1.

The occupancies of the two networks were set at 0.3, which approximately corresponds to the lowest occupancy of the water oxygens present in each network: water 610 in network 1 has the lowest occupancy of 0.26, while in network 2, water 428 has the lowest value of 0.3.

One asymmetric unit along the channel direction can be delineated by an approximate square region formed between the four hydroxyl groups of OR8 and OA17 that are shown in Fig. 4. Within this asymmetric unit, the two mutually exclusive water networks 1 and 2 can be observed [see Fig. 3(a)]. Fig. 4 shows the hydrogen bonding in the two networks: network 1, within the asymmetric unit (waters 225, 426, 214, 215, 228, 222, 427 and 610), is represented by the full-line hydrogen bonds [Fig. 4(a)], while network 2, again within this asymmetric unit (waters are drawn with dashed-line hydrogen bonds), is shown in Fig. 4(b). When going from one asymmetric unit to the next (above and below the square), what was the second network becomes the first and *vice versa*. To see the relative positions of both networks, see Fig. 3(a).

Further solvent networks can be formulated with occupancies of approximately 0.15, 0.15 and 0.1. One of these includes replacing waters 220, 224 and 225 in network 2 with an acetone molecule (occupancy *ca* 0.15). Several water molecules form part of more than one network. In the case of the waters in the pocket region (211, 212, 213, 216, 217, 223 and 418), these waters have unit occupancies and are present in all the networks in the 15 K structure. Other waters with lower occupancies participate in several or in only one network.

7. Covalent geometries

The covalent O—H bond lengths and H—O—H angles for each of the water molecules are listed in Table 1. Restraints were applied to the O—H bond lengths for the waters in the disordered interface and channel regions [0.96 (0.03) Å], but not for the waters in the highly ordered pocket region. Histogram distributions of the O—H distances and H—O—H angles are shown in Fig. 5. The mean O—H distance for all water molecules is 0.95 (0.04) Å [0.94 (0.04) and 0.95 (0.03) Å for the unrestrained and restrained geometries, respectively], which is within one standard deviation of the mean of 0.98 (0.02) Å for ice structures (Savage, 1986b), and also indistinguishable from the mean of 0.96 Å obtained for waters in small hydrates, determined by neutron diffraction (Chiari & Ferraris, 1982).

The H—O—H angles vary from 93 to 116° with a mean of 106.7 (5.6)° for all water molecules [110.3 (3.1)° for unrestrained and 105.1 (5.7)° for restrained geometries]. This distribution is tighter than in the 279 K analysis, where the range was 90–130° with a mean of 103°. The mean in the 15 K data is nearer to the means of 107° in the ices and small hydrate analyses.

8. Hydrogen-bonding geometries and coordination

The hydrogen-bonding geometries around each water molecule are listed in Table 1. X and Y refer to the polar O and N atoms of either the coenzyme B_{12} molecule (O

(a)

(b)

Fig. 5. Distributions of the covalent geometries of the water molecules in B_{12} coenzyme crystals at 15 K (N is the number of cases): (a) O—H distances and (b) H—O—H angles.

or N) or the water molecules (O only). Histograms for the individual hydrogen-bonding geometries are shown in Figs. 6(a)–(f).

8.1. $O(W) \cdots Y$ distances

The hydrogen-bond distances made by water molecules [O(W)] are listed in Table 1 and the histogram plotted in Fig. 6(a). They range from 2.49 to 3.27 Å with a mean value of 2.87 (0.17) Å for all waters [2.83 (0.12) for unrestrained and 2.89 (0.19) Å for restrained geometries]. For O(W)$\cdots$O distances only, the mean is 2.88 (0.18) Å. This compares with the mean distance of 2.88 (0.21) Å in the 279 K structure and 2.80 (0.10) Å for small molecular hydrates. The histogram also illustrates that contacts of less than *ca* 2.65 Å seem to be extremely unfavourable, and that the number of contacts above 2.9 Å tapers off rather gently. The point at 2.49 Å is the distance between the disordered waters 215 and 422. Further analysis may resolve this problem point. Fig. 6(b) shows the distribution of hydrogen-bond distances only between waters.

8.2. $O(W)$—$H \cdots Y$ distances

Fig. 6(c) is a histogram of the distribution of the $H \cdots Y$ distances for the hydrogen bonds made by water molecules. These distances are listed in Table 1. They are in the range 1.48–2.40 Å, with the mean being 1.95 (0.18) Å [1.93 (0.16) for unrestrained and 1.95 (0.16) Å for restrained geometries]. The mean $H \cdots Y$ distance in the 279 K structure is 1.91 Å. The mean O(W)—$H \cdots$O distances are 1.96 (0.18) and 1.86 (0.12) Å for the small crystal hydrates. The value of 1.48 Å is associated with the hydrogen bond between the problem waters 215 and 422. Fig. 6(d) shows the distribution of $H \cdots Y$ distances for the water molecules only.

8.3. X—$H \cdots Y$ hydrogen-bond angles

These are the angles subtended at the hydrogen in a hydrogen bond, listed in Table 1 and their distribution plotted in Fig. 6(e). The angles range from 135 to 176°, with the mean angle being 160.7 (10.2)° [163.1 (10.8) for the unrestrained and 159.6 (9.7)° for the restrained regions]. In the 279 K structure, the mean is 158°.

8.4. $X \cdots O(W) \cdots Y$ angles

Fig. 6(f) shows the distribution of the $X \cdots O(W) \cdots Y$ angles for all hydrogen bonds made by water molecules, that is to hydrogen-bond acceptors and donors. The angles range from 66.3 to 165.9°, with the mean being 108.5 (21.4)°. For the 279 K structure, the mean is 110°. The $X \cdots O(W) \cdots Y$ angles between water molecules and hydrogen-bond acceptors are listed in Table 1. The mean of the angles to acceptors is 108.5 (17.2)° and for small hydrates it is 107.6 (12.7)°.
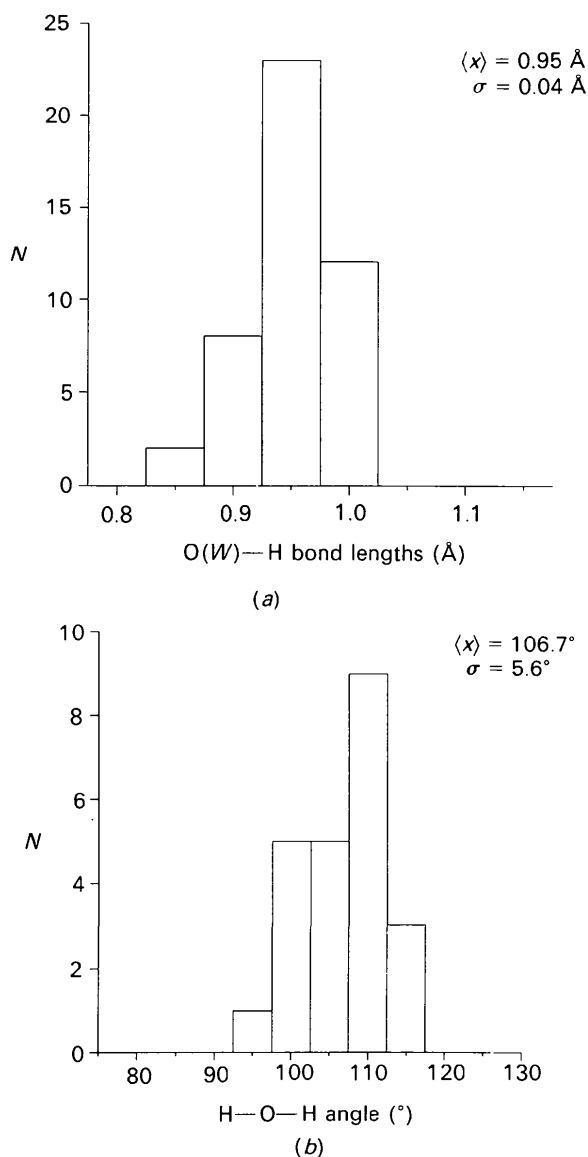
Table 1. *Water hydrogen-bond geometries between water molecules and between water molecules and polar groups of the coenzyme molecule (X and Y are either water O atoms or coenzyme polar atoms*

Coenzyme donors – water acceptors

X—H···O	X—H	X···Y	H···Y	X—H···Y
N40—D196···W212	1.01 (2)	2.99 (1)	2.06 (2)	152 (2)
N40—D197···W211	1.03 (2)	2.908 (8)	1.95 (2)	153 (2)
N52—H200···W214	1.02 (2)	2.90 (1)	1.96 (2)	152 (2)
N59—D136···W211	1.00 (1)	2.956 (9)	2.00 (1)	161 (1)
OR6—H206···W216	1.04 (2)	2.71 (1)	1.69 (2)	165 (2)
OA17—H208···W222	0.95 (4)	2.66 (2)	1.70 (4)	176 (4)
OA17—H298···W214	0.96 (5)	2.72 (1)	1.78 (5)	167 (5)

Water donors

O—H···Y	O—H	H—O—H	O···Y	H···Y	O—H···Y	X···O···Y
W211—H1···W217	0.97 (2)	110 (2)	2.79 (1)	1.83 (2)	168 (2)	
W211—H1···O68	0.94 (2)		3.02 (1)	2.28 (2)	135 (3)	84.6 (3)
W211—H2···O78			3.08 (9)	2.23 (2)	149 (2)	136.9 (3)
W212—H1···O33	0.89 (2)	110 (2)	2.91 (1)	2.08 (2)	155 (2)	
W212—H2···O62	0.94 (2)		2.98 (1)	2.06 (2)	169 (2)	84.3 (3)
W213—H1···O39	0.91 (2)	110 (2)	2.78 (1)	1.88 (22)	171 (2)	
W213—H2···O58	1.01 (2)		2.75 (1)	1.75 (2)	169 (2)	121.7 (4)
W216—H1···W217	0.92 (2)	105 (2)	2.87 (1)	2.01 (2)	156 (2)	
W216—H2···W220	0.99 (2)		2.78 (1)	1.80 (2)	168 (2)	113.9 (4)
W217—H1···W418	0.98 (2)	109 (2)	2.81 (1)	1.85 (3)	162 (2)	
W217—H2···O62	0.95 (2)		2.77 (1)	1.86 (2)	162 (2)	129.2 (4)
W223—H1···O44	0.89 (3)	116 (2)	2.71 (1)	1.82 (3)	173 (2)	
W223—H2···W213	0.83 (2)		2.70 (1)	1.87 (2)	176 (2)	112.6 (4)
W224—H1···W418	0.97 (3)	107 (3)	2.79 (2)	1.85 (3)	161 (2)	
W224—H2···W223	0.93 (3)		2.74 (2)	1.82 (3)	169 (3)	111.2 (7)
W418—H1···O39	0.92 (2)	112 (2)	2.84 (1)	1.97 (2)	157 (2)	
W418—H2···NA3	0.96 (2)		2.67 (1)	1.71 (2)	176 (2)	98.1 (4)
W220—H1···W224	0.94 (2)	108 (3)	2.75 (2)	1.82 (3)	173 (2)	
W220—H2···W229	0.99 (4)		2.82 (4)	1.87 (6)	161 (4)	95.5 (9)
W220—H1···W224		105 (3)				
W220—H3···W426	0.95 (4)		3.15 (4)	2.26 (5)	156 (4)	92.4 (8)
W214—H1···OA17	0.92 (3)	114 (3)	2.72 (1)	1.81 (3)	168 (3)	
W214—H3···W210	0.95 (3)		2.74 (2)	1.83 (3)	159 (2)	122.4 (6)
W214—H2···W215	0.94 (3)	101 (3)	2.83 (2)	1.98 (3)	151 (3)	
W214—H3···W428			2.78 (3)	1.87 (4)	160 (3)	125.8 (9)
W215—H1···NA3	0.96 (3)	105 (3)	2.85 (2)	1.93 (2)	158 (3)	
W215—H2···W214	0.94 (3)		2.83 (2)*	1.91 (3)	167 (3)	108.3 (6)
W215···W228			3.21 (3)			71.3 (5)
W225—H1···OR8	0.92 (3)	103 (4)	2.88 (2)	1.97 (2)	172 (3)	
W225—H2···W224	0.98 (5)		2.99 (3)	2.04 (5)	164 (5)	110.7 (7)
W431—H1···W422	0.97 (5)	99 (4)	2.95 (6)	2.05 (6)	152 (4)	
W431—H2···OA18	0.97 (5)		2.87 (4)	1.92 (3)	169 (4)	121 (2)
W428—H1···OR8	0.99 (5)	116 (4)	2.76 (4)	1.80 (5)	164 (5)	
W428—H2···W422	0.99 (3)		3.08 (5)	2.11 (5)	164 (3)	128 (2)
W210—H1···OR8	0.93 (3)	108 (3)	2.69 (2)	1.79 (3)	159 (3)	
W210—H2···W431	0.95 (4)		2.68 (4)	1.87 (5)	142 (3)	111 (1)
W227—H1···O51	0.97 (4)	109 (4)	2.87 (2)	1.94 (4)	159 (3)	
W227—H2···OA17	0.98 (4)		3.27 (2)	2.29 (4)	175 (4)	113.7 (7)
W422—H1···W215			2.49 (4)	1.48 (4)	176 (4)	
W422···W229			3.27 (6)			87 (1)
W228—H1···W210	0.94 (3)	101 (3)	2.99 (3)	2.05 (2)	174 (2)	
W228—H2···W225	0.98 (4)		3.16 (3)	2.21 (4)	161 (3)	85.7 (8)
W610—H1···W427	0.98 (6)	102 (6)	2.98 (5)	2.09 (6)	151 (5)	
W610—H2···W428	0.85 (6)		2.70 (6)	1.90 (5)	155 (5)	134 (2)
W222—H1···W228	0.96 (3)	93 (3)	2.77 (3)	1.86 (3)	158 (3)	
W222—H2···W610	0.95 (4)		2.83 (5)	1.93 (6)	156 (4)	124 (1)
W226—H1···O51	0.96 (6)	111 (5)	2.66 (3)	1.80 (5)	147 (5)	
W426—H2···W225	1.01 (5)		2.90 (4)	1.99 (4)	148 (4)	97 (1)
W427—H1···W426	0.92 (4)	100 (4)	3.02 (4)	2.26 (5)	141 (4)	
W427—H2···OA18	0.95 (9)		3.18 (3)	2.40 (8)	139 (7)	100.1 (9)

* Repeated values.

8.5. Hydrogen-bond coordination

The hydrogen-bond coordinations range from 2 to 5. In network 1: nine (53%) of the waters have a coordination of 3, seven (41%) of 4 and one (6%) of 5. For network 2: three waters (18%) have a coordination of 2, seven (41%) of 3, six (35%) of 4 and one (6%) of 5. The coordination 5 is attributed to water 211, which is situated in a polar environment, with one of its H atoms capable of forming a bond with a phosphate O atom (OP2) and a hydroxyl group on the ribose (OR7) [Fig. 3(a)]. The coordination of 2 in network 2 is due
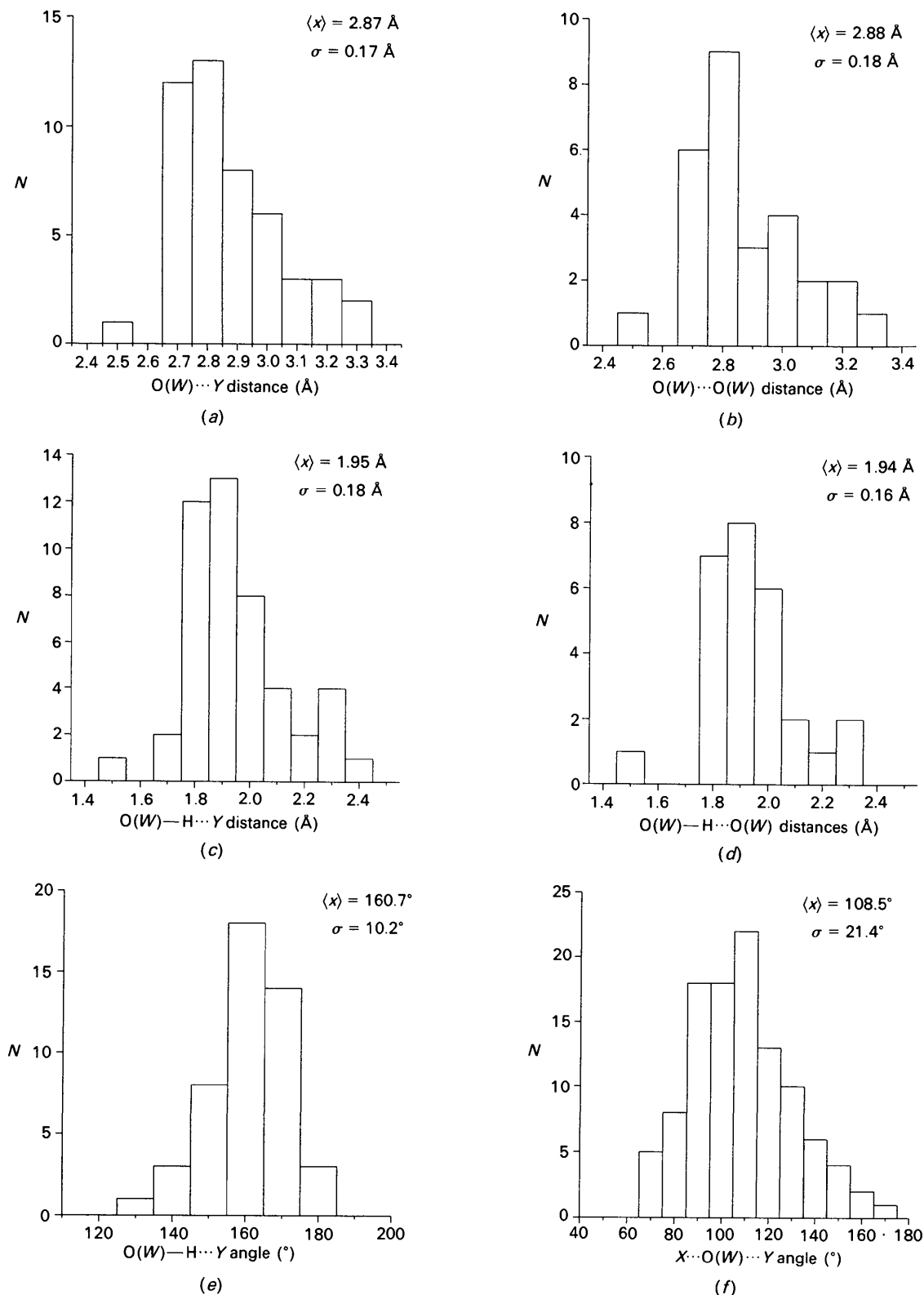
Fig. 6. Distributions of the water–water and water–coenzyme hydrogen-bond geometries at 15 K (where X and Y are either water O atoms or coenzyme polar atoms, and N the number of cases): (a) O(W)$\cdots Y$, (b) O(W)$\cdots$O(W), (c) H(W)$\cdots Y$ and (d) H(W)$\cdots$O(W) hydrogen-bond lengths, (e) O(W)—H$\cdots Y$ and (f) $X\cdots$O(W)$\cdots Y$ hydrogen-bond angles.

to waters 227 and 225, where there are no hydrogen-bond donors pointing towards the oxygen lone pairs, and water 220, where one H atom does not seem to form a hydrogen bond. The $X \cdots O(W) \cdots X$ hydrogen-bond angles range from 70 to 137°, where X is a water O atom or a coenzyme polar atom. This range is similar to those found for water hydrogen-bond coordinations in known ice structures and small hydrate crystals.

9. Interactions with apolar groups

Two types of water interactions with apolar groups of the coenzyme molecule can be seen in the crystal. One involves forming short – possibly of weak hydrogen-bonding character – interactions directly with several C—H groups and the other in forming partial clathrate cage-like structures around various apolar groups.

9.1. Short contacts between C—H groups and water molecules

A number of C—H$\cdots$O(W) contacts are present in the coenzyme crystals at distances less than the expected van der Waals radius sum. Using as a selection criterion an H$\cdots$O(W) cut-off distance of 2.7 Å and 90° for the C—H$\cdots$O(W) angle (Steiner & Saenger, 1992), six short C—H$\cdots$O(W) contacts occur, and are listed in Table 2. The waters involved are 213, 223, 418, 222 and 610, with C$\cdots$O(W) distances ranging from 3.16 to 3.56 Å. Two of these C—H$\cdots$O(W) hydrogen bonds to waters 213 and 222 were previously noted in the 279 K D_2O analysis (Savage, 1983).

Waters 213, 223 and 418 lie in a fairly apolar region in the pocket region, intermixed with coenzyme polar atoms. Waters 222 and 610 are part of the water networks in the channel region. For waters 213, 223 and 222, the C—H group points almost directly to the lone-pair regions, with quite straight C—H$\cdots$O(W) angles (160, 160 and 170°, respectively) and short H$\cdots$O(W) distances (2.27, 2.33 and 2.29 Å, respectively). All three of the interactions are present in the 279 K model. The geometries of the C—H$\cdots$O(W) interactions involving waters 418 and 610 are somewhat looser.

Such short contacts of mixed polar–apolar character have been noted before in detailed studies of local environments in proteins. Finney (1978) noted that in RNase-S, some 40% of the internal interactions could be classified as of mixed polar–apolar nature. Later work on insulin – at that time one of the best resolved protein crystal structures – showed (Finney, Gellatly, Golton & Goodfellow, 1980) a clear tendency for these polar–apolar contacts to lie at distances (3.0–3.5 Å) significantly shorter than the van der Waals' radius sum (variously estimated as between 3.7 and 4.0 Å). The higher resolution data presented here for the B_{12} coenzyme confirm the tentative conclusions drawn in this earlier work. As also more recently noted by Steiner

Table 2. *Water hydrogen-bond geometries between water molecules and* C—H *groups of the coenzyme molecule*

C—H$\cdots$O	C—H	C$\cdots$Y	H$\cdots$Y	C—H$\cdots$Y
CR7—H144$\cdots$W213	1.11 (2)	3.34 (1)	2.27 (2)	160 (1)
C49—H130$\cdots$W223	1.11 (2)	3.39 (1)	2.33 (2)	160 (1)
C36—H170$\cdots$W418	1.11 (2)	3.16 (1)	2.40 (2)	124 (1)
C86—H148$\cdots$W222	1.09 (1)	3.37 (2)	2.29 (2)	170 (1)
C66—H139$\cdots$W213	1.10 (1)	3.56 (1)	2.54 (2)	155 (1)
C74—H140$\cdots$W610	1.12 (1)	3.53 (4)	2.50 (4)	154 (1)

& Saenger (1993), these short contacts are found in positions where, were a normal proton donor present, a hydrogen bond to the water oxygen would be possible. The energetic contribution these short polar–nonpolar contacts might make was estimated earlier to be small, but possibly of some significance, at the level *ca* 0.5 kcal mol^{-1} (Finney, Gellatly, Golton & Goodfellow, 1980). Taking a 'standard' hydrogen bond as contributing around 5 kcal mol^{-1}, the C—H$\cdots$O(W) interaction might 'retrieve' perhaps 10% of the stabilization that the 'lost' hydrogen bonds would have provided. Although this may be helpful in maintaining local stability, the quantitative contribution appears relatively small [approximately twice that from the van der Waals' contribution for the two interacting groups (Finney, Gellatly, Golton & Goodfellow, 1980)], and we would caution against overstressing the role of these short polar–nonpolar contacts. Labelling them as C—H$\cdots$O 'hydrogen bonds' is likely to overemphasize their strength and we prefer not to use this term.

9.2. Partial 'clathrate-like' water structures

Many of the coenzyme B_{12} regions (shaded in Figs. 2–4) contain a number of apolar groups and several examples of partial 'clathrate-like' water cages are apparent. A complete layer of apolar groups containing no polar atoms (NA7 is above) lies underneath the five-membered ring of waters (217, 216, 220, 224 and 418) in the pocket region [apolar groups under the water ring are not shown in Fig. 3(a) for reasons of clarity]. This ring forms a hydrogen-bonded network of waters reminiscent of a partial cage of water structure. No short C—H$\cdots$O(W) interactions are made from the apolar layer below to the five-membered ring of waters. In Fig. 4(a), a larger partial cage also occurs around one of the methyl groups (CB10) of the benzimidazole group. In this case, about ten water molecules are involved which can form several five- and six-membered water rings and other continuous hydrogen-bonded networks. The partial cage extends from water 216 to water 220, adjacent to the benzene ring of the benzimidazole group, and then around the methyl group to the waters in the channel, where there are two alternative water network structures: networks 1 and 2. In network 1, the partial cage continues to waters 426, 427, 215, 228, 222, 610,

214, 428 and 422, whilst in network 2, it continues with waters 422, 215, 431, 214, 210, 227, 228 and 222.

The water molecules in these incomplete 'clathrate-like' cages have hydrogen-bond coordinations mostly of 3 and 4. One or two have coordinations as low as 2. For example, water 227, which lies at the bottom of the channel, forms two hydrogen bonds with its H atoms to coenzyme polar atoms (see Table 1), but no hydrogen bonds are made to the acceptor region of this water, either from other water molecules or polar coenzyme groups. The shortest potential C—H···O(W) hydrogen bond to this water is 3.9 Å away.

It appears that the environments of the water molecules in the coenzyme crystals are being optimized to form as many hydrogen bonds as possible with adjacent polar groups of other waters or the coenzyme molecule. Around apolar groups, the geometry of water–water interactions naturally leads to the partial cages observed. Where potential hydrogen bonds to water molecules are unfulfilled, direct interactions to adjacent coenzyme C—H groups may occur if the local geometries are favourable.

10. Short-range structure: non-bonded contacts

In addition to attractive hydrogen-bonding forces that hold the water molecules together, non-bonded interactions of the repulsive type also occur which prevent the structures from collapsing. Details of the short-range contacts of O···O, H···O and H···H have been examined in ice and small hydrate structures (Savage & Finney, 1986; Savage 1986a, 1993) and four repulsive regularities (named RR1–4) were characterized, of which we consider RR1 here.

The RR1 regularity relates to the O···O repulsion in a hydrogen bond. In standard plots of the O—H···O hydrogen-bond angle versus the H···O hydrogen-bond length, a regression line is usually drawn on the plot to represent an overall decrease in the angle as the distance increases [Fig. 7(a)]. The scatter of the geometries is too much outside the precision of the data points (ca 0.02 Å and < 1.0°), for a correlation to be significant. Also, some long hydrogen bonds are very straight (180°) and some short bonds very bent.

Fig. 7(b) shows the same plot as in Fig. 7(a), but for water hydrogen bonds in ices and small hydrates analysed by neutron diffraction. It appears that hydrogen bonds can bend when required, but there is a limit on the amount of bending and this is represented by the full lines in Figs. 7(b) and (c). This line is in effect the hydrogen-bond bending limit curve. The hydrogen-bond geometries of the waters in the 15 K analysis are shown in Fig. 7(c). Two points lie within 1.5σ below the hydrogen-bond limit line, and hence do not constitute a major violation of RR1. These are the hydrogen bonds between waters 210 and 431 and the

hydrogen bond between waters 426 and O51. The actual hydrogen-bond angles and distances a water hydrogen bond may have appear to depend on the local packing arrangements determined by the surrounding short-range
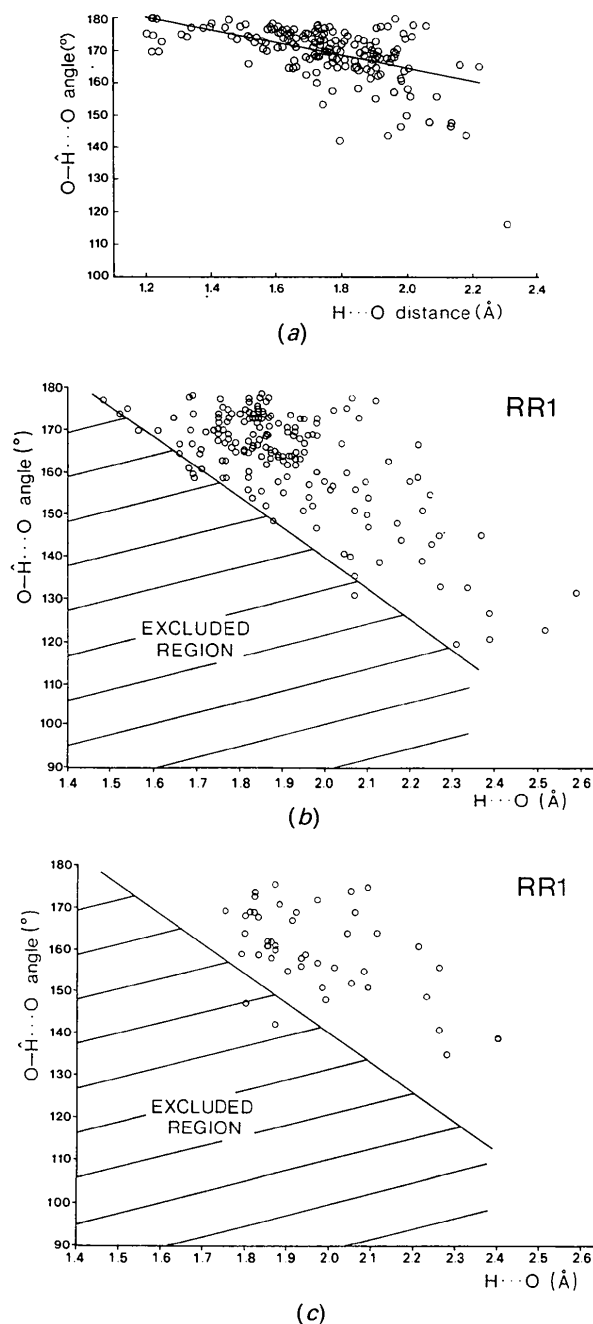

(a)

(b)

(c)

Fig. 7. (a) Standard hydrogen-bond geometry plot of the O—H···O hydrogen-bond angles as a function of the distance H···O (from Olovsson & Jonsson, 1976). (b) RR1 plot for water molecules from an analysis of water geometries in ices and small hydrate crystals (Savage & Finney, 1986). (c) RR1 plot for water molecules in the 15 K coenzyme structure.

contacts of the RR2 (non-hydrogen-bonded O···O), RR3 (non-hydrogen-bonded H···O) and RR4 (H···H) regularities. The characteristics of these interactions will be given in a more detailed analysis of the solvent networks.

11. Discussion and concluding remarks

Overall, the intermolecular geometry of the basic water structure within coenzyme B_{12} crystals is similar to those in the known ice structures and in small hydrates of biomolecules. A wide range of hydrogen-bond geometries is observed. Omitting the short hydrogen-bond distance between waters 422 and 215, the O···OH distances vary from 2.67 to 3.27 Å. This is significantly larger than the range 2.73–2.92 Å in the ice polymorphs, but similar to the 2.6–3.2 Å range in small hydrates.

The ranges 1.71–2.40 Å for H···O hydrogen-bond distances and 135–176° for the O(W)—H···Y hydrogen-bond angles are also similar to those in small hydrate structures, but the distributions are not as tight as in the ice polymorphs, which are 1.72–1.91 Å and 150–180°. The spread in X···O(W)···Y hydrogen-bond angles of the waters in the ice polymorphs is 70–144°. In small hydrates, the spread is somewhat larger at 76–150°, while in this analysis the spread increases to 70–165°.

The hydrogen coordination of the waters varies from 2 to 5, with most waters having values of 3 or 4. Values of 2 and 5 are usually associated with waters that are either in areas rich in apolar or polar atoms, respectively. Some three-centred or bifurcated hydrogen bonds are formed: these include waters 211 and 427.

With respect to the maximization of the hydrogen-bonding donor potential, ca 97% of the water H atoms are able to form hydrogen bonds with acceptor atoms: 34/34 for network 1 and 32/34 for network 2. This figure is 100% for the ice polymorph structures.

In the case of the acceptor lone-pair regions of the coenzyme waters, the maximization is somewhat less. Assuming a potential maximum of two hydrogen bonds to each lone pair region of a water molecule, then only ca 75% of the water acceptor hydrogen-bonding capacity is fulfilled: 27/34 for network 1 and 24/34 for network 2. Thus, a significant number of potential hydrogen bonds are not formed to the acceptor regions: 17 hydrogen bonds not made between the two networks. When the short CH···O(W) contacts in Table 2 are taken into consideration and added as interactions directed towards lone pairs, the number of interactions not made to the acceptor regions is reduced to 13, which corresponds to an 80% maximization of the acceptor interactions with 'donated' protons. Recalling from the earlier discussion that each of these is unlikely to contribute at the level of more than 10% of a hydrogen bond to the local stability, these short polar–apolar contacts do not appear to enhance the overall stability of the system more than marginally.

Over recent years, high-resolution studies of water organization in hydrate crystals have greatly improved our understanding of the geometry of water interactions, both with other water molecules and with polar and non-polar groups on neighbouring molecules (Savage, 1986a,b; Savage & Finney, 1986). Relying in particular on neutron scattering results, which allow unambiguous location of H atoms and hence of water orientation, a number of regularities have been identified which have allowed us to rationalize with increasing confidence the solvent organization in different environments.

The results presented here represent the largest system yet studied with respect to the high resolution, low temperature and precision of the data. What we have found is consistent with what we have learned from earlier studies. Not only is this consistency welcome, but it confirms our improved understanding of the structural principles that control water geometries, e.g. in hydrating biomolecules. This body of work thus equips us with tools that can be used with increased confidence in a variety of ways, for example, in restraining solvent in protein crystal refinement. It also, we believe, helps us further towards demystifying the contribution of solvent to the stability and interactions of biomolecules.

Some interesting questions do, however, remain. Despite the low temperature, the fact that some – albeit reduced with respect to room temperature – disorder in the channel remains is of some interest. This remaining disorder suggests that, in this system at least, the water itself may not be able to fully order in the sense of forming only a single network. Whether this is because the geometry of the channel environment is inconsistent with full ordering (by which we mean a single water network) or because more than one network can be constructed consistent with the geometry of the groups lining the channel is not clear, but is perhaps an interesting speculation. The disposition of these groups may perhaps be thought of as forcing the system to make a variety of attempts to minimize disruption through, for example, variations in coordination number, and of distances and angles. The fact that relatively weak polar–non-polar interactions can be identified through short contacts suggests further that the system does what it can locally to maximize the interactions that can be made in the absence of the possibility of hydrogen bonding, even though the energetic contribution of each of these weak interactions may be quantitatively very small.

Further light on these issues might be shed by extending this study to even higher resolution (there is much data further out), and perhaps by reducing the temperature even further.

References

BETZEL, C., SAENGER, W., HINGERTY, B. E. & BROWN, G. M. (1984). *J. Am. Chem Soc.* **106**, 7545-7557.

BOUQUIERE, J. P., FINNEY, J. L., LEHMANN, M. S., LINDLEY, P. F. & SAVAGE, H. F. J. (1993). *Acta Cryst.* B49, 79-89.

CHIARI, G. & FERRARIS, G. (1982). *Acta Cryst.* B38, 2331-2341.

DAUTER, Z., SIEKER, L. C. & WILSON, K. S. (1992). *Acta Cryst.* B48, 42-59.

DRIESSEN, H., HANEEF, M. I. J., HARRIS, G. W., HOWLIN, B., KHAN, G. & MOSS, D. S. (1989). *J. Appl. Cryst.* **22**, 510-516.

FINNEY, J. L. (1978). *J. Mol. Biol.* **119**, 415-441.

FINNEY, J. L., GELLATLY, B. J., GOLTON, I. C. & GOODFELLOW, J. M. (1980). *Biophys. J.* **32**, 17-33.

JEFFREY, G. A. & MALUSZYNSKA, H. (1990). *Acta Cryst.* B46, 546-549.

LINDLEY, P. F., NAJMUDIN, S., BATEMAN, O., SLINGSBY, C., MILES, D., KUMARASWAMY, V. S. & GLOVER, I. (1993). *J. Chem. Soc. Faraday Trans.* **89**, 2677-2682.

MASON, S. A., BENTLEY, G. A. & McINTYRE, G. J. (1984). *Neutrons in Biology*, edited by B. P. SCHOENBORN, pp. 323-334. New York: Plenum Press.

OLOVSSON, I. & JONSSON, P. G. (1976). *The Hydrogen Bond*, Vol. 2, edited by P. SCHUSTER, G. ZUNDEL & C. SANDORFY, p. 393. Amsterdam: North-Holland.

PHILLIPS, D. C. (1966). *Sci. Am.* **215**, 78-90.

SAVAGE, H. F. J. (1983). PhD Thesis, Univ. of London.

SAVAGE, H. F. J. (1986a). *Biophys. J.* **50**, 947-980.

SAVAGE, H. F. J. (1986b). *Water Science Reviews*, Vol. 2, edited by F. FRANKS, pp. 67-148. Cambridge: Cambridge Univ. Press.

SAVAGE, H. F. J. (1993). *Water and Biological Macromolecules*, edited by E. WESTHOF, pp. 3-44. London: MacMillan.

SAVAGE, H. F. J. & FINNEY, J. L. (1986). *Nature (London)*, **322**, 717-720.

SAVAGE, H. F. J., LINDLEY, P. F., FINNEY, J. L. & TIMMINS, P. A. (1987). *Acta Cryst.* B43, 280-295.

SHELDRICK, G. M. (1976). *SHELX76. Program for Crystal Structure Determination.* Univ. of Cambridge, England.

STEINER, T., MASON, S. A. & SAENGER, W. (1990). *J. Am. Chem. Soc.* **112**, 6184-6190.

STEINER, T., MASON, S. A. & SAENGER, W. (1991). *J. Am. Chem. Soc.* **113**, 5675-5687.

STEINER, T. & SAENGER, W. (1992). *J. Am. Chem. Soc.* **114**, 10146-10154.

TEETER, M. M. & HOPE, H. (1986). *Ann. N. Y. Acad Sci*, **482**, 163-165.

TEETER, M. M. & WHITLOW, M. D. (1986). *Trans. Am. Crystallogr. Assoc.* **22**, 75-88.

ZABEL, V., SAENGER, W. & MASON, S. A. (1986). *J. Am. Chem. Soc.* **108**, 3664-3673.

Ab Initio Structure Determination From Powder Data Using Direct Methods

BY R. SPENGLER, H. ZIMMERMANN AND H. BURZLAFF

Institut für Angew Physik, Lehrstuhl für Kristallographie, Bismarckstrasse 10, 91054 Erlangen, Germany

AND J. JANSEN, R. PESCHAR AND H. SCHENK

Laboratorium voor Kristallografie, Universiteit van Amsterdam, Nieuwe Achtergracht 166, 1018 WV Amsterdam, The Netherlands

Abstract

An *ab initio* structure determination was carried out on the basis of powder data using the programs developed by Jansen, Peschar & Schenk [*J. Appl. Cryst.* (1992a), **25**, 231-236; *J. Appl. Cryst.* (1992b), **25**, 237-243; *Z. Krist.* (1993), **206**, 33-43]. The results give a very good approximation to the single crystal structure. The main problems in structure determination from powder data so far are the determination of the correct space group and a better possibility than Rietveld refinement to refine the structural model coming out of the direct methods.

1. Introduction

In cooperation with the Department of Chemistry at the University of Ioannina and the Institute of Geology and Mineral Exploration in Athens, a structure determination was carried out on a series of metallochloranilate compounds. These compounds show a very high grade of twinning, as well as absorption effects. In general, it is impossible to select non-twinned single crystals large enough for data collection on a four-circle diffractometer.

As a first example for *ab initio* structure determination from powder data, the compound disodium bis[3,6-dichloro-4,5-dihydroxy-3,5-cyclo-hexadiene-1,2-dionato(2−)] dioxouranium hexahydrate (Bram *et al.*, 1994) was selected. The pattern of the sample is rather complex, as well as the structure, which contains 22 atoms in the asymmetric unit.

Structure determination by powder data was attempted using two methods, Patterson (Brüderl *et al.*, 1994) and direct methods. To fit the powder pattern and separate overlapping intensities, the programs developed by Jansen, Peschar & Schenk (1992a,b, 1993) were used for optimal symbolic addition. In the subsequent calculations, the *Xtal*3.0 system (Hall & Stewart, 1990) was used.